

SIMULATION OF AND PROGRESS TOWARDS A MICRON-SCALE LASER-POWERED DIELECTRIC ELECTRON SOURCE*

G. Travish, J. B. Rosenzweig, Jin Xu, UCLA, Los Angeles, CA 90095, U.S.A.

R. B. Yoder, Manhattanville College, Purchase, NY 10577, U.S.A.

S. Boucher[#], RadiaBeam Technologies LLC, Marina del Rey, CA 90292, U.S.A.

Abstract

A dielectric, slab-symmetric structure for generating and accelerating low-energy electrons has been under study for the past two years. The resonant device is driven by a side-coupled laser and is configured to maintain field profiles necessary for synchronous acceleration and focusing of nonrelativistic particles. Intended applications of the structure include the production of radiation for medical treatments, imaging, and industrial uses. Results from 3D simulation of the structure geometry and its resonant properties are presented here.

INTRODUCTION

A dielectric-based slab-symmetric accelerator module, resonantly excited by a side-coupled laser pulse, was first described in 1995 [1] and has been investigated in various wavelength regimes [2]. This concept has been extended more recently to the non-relativistic domain, allowing the development of a laser-powered particle source capable of producing electron beams of a few MeV in a resonant structure having overall dimensions of ~mm or less per side. The structure is constructed from dielectric layers using micromachining methods common in the integrated-circuit industry. The theory of these trans-relativistic microaccelerators has been briefly described previously [3], and experimental testing of a sample structure is in progress—initially, a simplified version with constant, speed-of-light phase velocity. In this paper, we describe detailed simulation results of sample structures and progress toward testing a prototype.

Description of the Structures

There are several versions of this microaccelerator. Figure 1 shows a typical example described in the literature, containing a pair of dielectric slabs on either side of a vacuum gap, with a metal layer on the outer surface of each slab. Periodic slots in at least one metal layer have the dual function of coupling laser light into the structure and constraining the structure to resonate in a synchronous accelerating mode. The structure is powered by a laser having $\lambda = 800$ nm, which sets the overall scale of the device.

As no real metal is a near-perfect conductor in this wavelength range, the laser will penetrate the metal somewhat, resulting in ohmic losses and decreased structure Q , as well as lowered breakdown limits and

perturbation in the field shape. For this reason, the ultimate high-power version of this accelerator will replace the metal walls with a dielectric mirror or Bragg stack, with modulation of the inner stack layers (rather than slots) producing the synchronous mode. (This structure will be optimized in future work.) However, for our initial proof-of-principle experiments, we can exploit the dielectric response of the metal to construct a resonant all-metal structure that is extremely simple to construct and test. It should be noted that “extraordinary transmission” through periodic arrays of sub-wavelength holes and slots has been intensively studied in recent years [4, 5].

In the all-metal test structure, the dielectric layer lining the vacuum gap in Fig. 1 is simply omitted; the vacuum gap is then bounded by slotted metal layers, each mounted on an external thick substrate. The acceleration performance of this structure would be poor, but it will still be possible to verify the physics and benchmark simulations using this version of the accelerator, and such a test would represent the first laboratory measurements of any slab-symmetric laser-driven structure.

Structure Parameters

The frequency of the resonant accelerating mode for the metal/dielectric structure is controlled by several elements of the structure geometry: the vacuum gap spacing ($2a$), the thickness ($b - a$) of the metal layer, and the dielectric constant ϵ of the substrate slab. (See Fig. 1.) In addition, the coupling slot periodicity must equal the laser free-space wavelength λ . The structure resonance is then tuned to match the frequency of the drive laser. In practice, once the device is constructed, the gap spacing a can be adjusted, via e.g. a nanopositioning stage with active feedback, to tune the resonance.

The dimensions and shape of the coupling slots affect the coupling Q (and hence the peak field reached) and, in general, perturb the resonant frequency and fields. Slot height h (equivalent to the thickness of the metal layer) and width w are the main parameters. In the ideal case of a perfectly conducting metal, a slot depth of $\lambda/4$ leads to zero field perturbation, but with typical (real) conductors the losses in such a slot are too large to be tolerated.

The all-metal structure uses the dielectric properties of metal at this wavelength to substitute for the dielectric layer altogether, with the slots being filled with vacuum, not dielectric. In that case, the resonance is controlled entirely by the gap spacing and the electromagnetic properties of the metal.

*Work supported in part by US DoE and by grants from UCLA.

[#]boucher@radiabeam.com

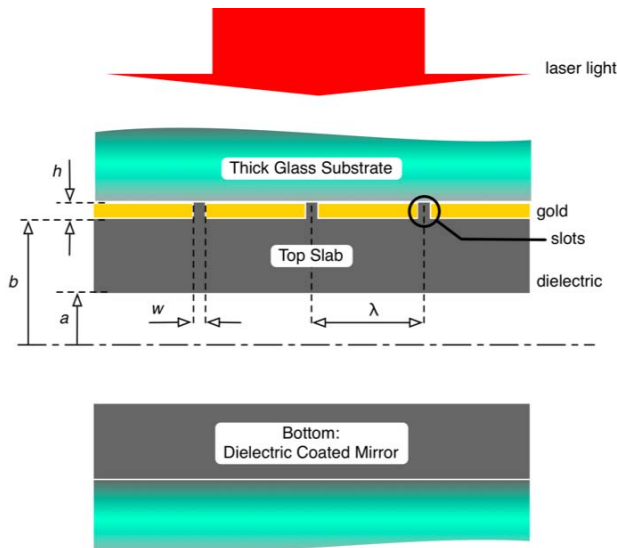


Figure 1: Structure layout and dimensions for a dielectric/metal structure. (The all-metal structure is similar, but omits the dielectric below the gold layer.)

SIMULATION RESULTS

Simulations were carried out using two 3D finite-difference electromagnetic codes, HFSS (Ansoft, Inc.) and CST Microwave Studio, including both frequency and time domain. Simulation goals were to establish optimal values for the design parameters described above, to determine the allowable tolerances in each, and to predict useful diagnostics for experimental test.

A complete accelerator, which consists of hundreds of structure periods, is impractical to simulate. The conclusions shown here are based on simulation a single period (with periodic boundary conditions). In practice, we are only able to simulate some 10 periods. The size of the structure overall (i.e. the overall width and length of the accelerator) is best optimized through experimental test.

Field Optimization

Once the dielectric thickness and constant have been chosen, the coupling geometry can be optimized, with adjustment of the vacuum gap spacing to compensate for small mistunings associated with the slots. Figure 2 shows the significant alteration in the fields when perfectly conducting metal is replaced by gold, in a computational model that allows for appropriate real and imaginary dielectric parameters for the metal [6]. The ratio of field strength on axis to that of the incoming laser is reduced from 3.8 to 1.4, due to decreasing ohmic Q as well as losses in the coupling slots. This illustrates the need for an all-dielectric structure in the final device; our cold testing begins with metal only as a convenient first verification of the simulations.

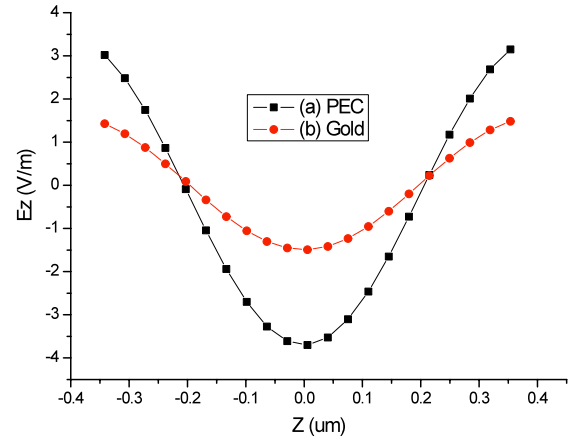


Figure 2: For the metal+dielectric design, comparison of resonant axial field E_z for two structures of identical dimensions. (a) perfectly conducting metal boundary; (b) gold boundary, including losses. (HFSS simulation)

The table below lists the optimal values determined by parameter scans, with their associated tolerances, for the metal-walled dielectric structure having a vacuum gap spacing of 800 nm. The performance is particularly sensitive to the height h of the coupling slots; the optimal value represents a compromise between high losses for large h and unacceptable field perturbation for small h .

Table 1: Optimized dimensions and tolerances, dielectric/metal structure.

Parameter	Nominal value	Tolerance
Overall slab width	200 μm	$\pm 50 \mu\text{m}$
Overall slab length	1000 μm	$\pm 100 \mu\text{m}$
Slab thickness ($b-a$)	38.6 nm	$\pm 1 \text{ nm}$
Slot width (w)	50 nm	$\pm 10 \text{ nm}$
Slot height (h)	80 nm	$\pm 5 \text{ nm}$
Dielectric constant (ϵ)	6.8	± 0.5

The expected field profile for an all-metal test structure is shown in Figure 3. Note that field on axis is comparable to that of the drive laser (normalized to 1 V/m in the simulations and represented by light-green). For the all-metal structure, the dimensions are determined by the available construction methods at UCLA. The test structure is etched in an $\sim 100\text{-nm}$ gold layer deposited on a fluid-jet polished sapphire substrate. An array of roughly 120 slots, each 30 μm long and 30 nm wide, and spaced 800 nm apart, is then cut into the gold using focused-ion-beam milling. As it is impossible to fabricate these slots with perfectly perpendicular walls, we therefore include the effects of angled slot walls.

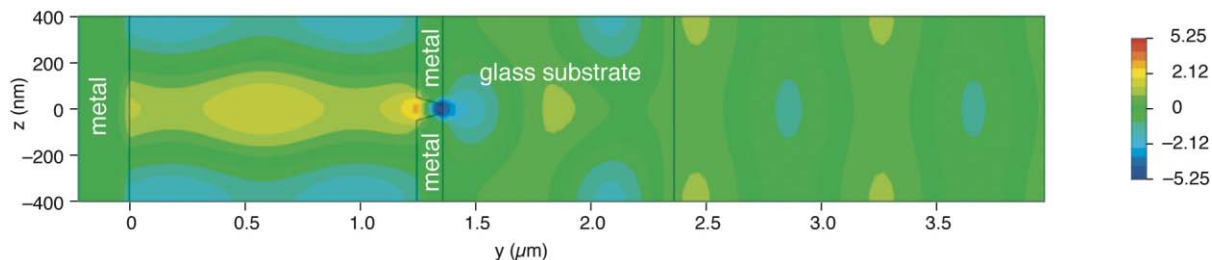


Figure 3: Expected field profile (E_z) in V/m for an all-metal structure, $x=0$ plane (CST MWS simulation), normalized to a 1 V/m drive laser field. The laser propagates from the right (+y) and beam propagation is from $-z$ to $+z$, through the vacuum gap (left third of figure). The coupling slot narrows from 140 nm to 40 nm at the substrate end.

Fig. 3 shows that this simplified structure results, among other things, in distortion of the wavefronts. The invariance of fields in the narrow (y) direction is lost when all-metal is used, and a small y -dependent phase shift is introduced, visible in the figure as a ‘Coke-bottle’ shape in the field profile. While such fields would be deleterious to a particle beam, the existence of the resonance can still be verified and documented using low-power cold testing.

S Parameters

The quality of the resonances can be diagnosed through measurement of the S_{11} and S_{12} parameters for this system. S_{11} measurements can be performed using a beam splitter on the incoming laser beam, allowing for diagnosis of the reflected signal; likewise, any power coupled out through the bottom of the structure (via slots or simply an imperfect metal mirror) can be used for an S_{12} signal.

We have found that a preliminary test of slot performance may be obtained from taking S_{11} and S_{12} measurements on the upper layer alone (i.e., the top half of the accelerator structure), as the periodicity of the slots is sufficient to produce spectral information in the signal.

Figure 4 shows sample S -parameter scans simulated using HFSS.

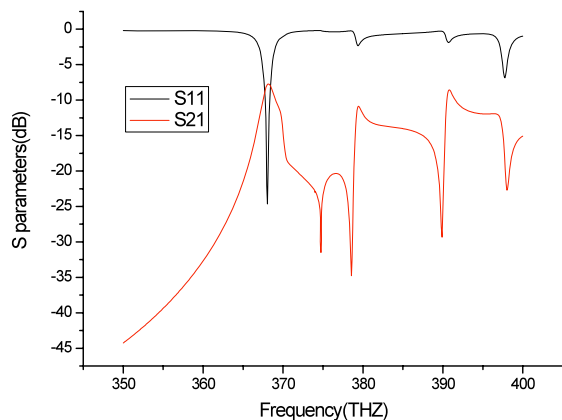


Figure 4: S parameters for the all-metal structure. (HFSS simulation)

CONCLUSION

The simulations described here show that a useful cold test of this microaccelerator principle can be carried out using S_{11} and S_{12} measurements on two varieties of simple metal- and dielectric-based structures. These tests are the first experimental investigation of a slab-symmetric resonant structure, and an important first step in the development of a nonrelativistic microaccelerator module.

ACKNOWLEDGMENTS

The authors wish to thank Noah Bodzin and Steve Franz for their guidance on structure fabrication; and, Nick Barov and Brendan O’Shea for early assistance with simulations.

REFERENCES

- [1] J. Rosenzweig, A. Murokh, and C. Pellegrini, *Phys. Rev. Lett.* **74**, 2467 (1995).
- [2] A. Tremaine, J. Rosenzweig, and P. Schoessow, *Phys. Rev. E* **56**, 7204 (1997); R. B. Yoder and J. B. Rosenzweig, *Phys. Rev. ST–Accel. Beams* **8**, 111301 (2005).
- [3] R. B. Yoder, G. Travish, and J. B. Rosenzweig, *Proceedings of PAC2007*, pp. 3145–3147.
- [4] Y. Xie *et al.*, *Opt. Express* **14**, 6400 (2006).
- [5] R. Biswas *et al.*, *J. Opt. Soc. Am. B* **24**, 2589 (2007).
- [6] A. D. Rakic *et al.*, *Appl. Optics* **37**, 5271 (1998); *Appl. Optics* **22**, 1099 (1983).